Suomi NPP VIIRS Detector Dependent Relative Spectral Response Variation Effects using Line-by-Line Radiative Transfer Model Calculations

Zhuo Wang[a] and Changyong Cao[b]

[a] University of Maryland, College Park, Maryland, [b] NOAA/NESDIS/STAR, College Park, Maryland

Abstract

The Visible Infrared Imaging Radiometer Suite (VIIRS) is a modern focal plane array based satellite radiometer, which has many detectors with slightly different relative spectral response (RSR). Effect of RSR differences on imaginary artifacts, as well as geophysical retrieval uncertainties has not been well studied. Previous studies used the MODTRAN model for detector-level radiance simulations. However, it is limited by the spectral resolution of the model relative to the narrow spectral bandwidth of the detectors. This study evaluates detector level RSR using Line-by-Line Radiative Transfer Model (LBLRTM) at higher spectral resolution 0.01 cm^{-1} for VIIRS bands M15 and M16 under different atmospheric conditions. From the model simulation and case studies of VIIRS SDR brightness temperature data, we found that the striping in imagery is most likely related to the difference between band averaged and detector level RSR, which has some atmospheric dependency. Cumulative histogram method is utilized to quantify the striping. These findings will help S-NPP and J1 to better understand the impact of the difference in detector-to-detector RSR on VIIRS geophysical retrieval and reduce the uncertainties.

Background

Previous studies have been performed to identify the possible causes for SST striping issue [*Padula and Cao, 2015*]. They used MODTRAN model to simulate the spectral radiance at the spectral resolution of 1cm^{-1} for five standard atmospheric profiles. Their results indicate that the SST product is likely affected by small differences in detector-level SRF, and the detector-to-detector differences have small atmospheric dependence.

A study from SST EDR team [*Dash and Ignatov, 2008*] evaluated the biases in the top-of-atmosphere (TOA) brightness temperature (BT) modeled with MODTRAN model. They concluded that MODTRAN brightness model does not reproduce spectral, angular, and water vapor dependencies with accuracies acceptable for SST analyses. Therefore, in this study, we use LBLRTM with higher resolution to investigate the SST striping issue.

VIIRS Daytime SST Algorithm & Imagery Analysis

The daytime VIIRS SST is computed from a non-linear split window algorithm using the brightness temperatures from bands M15 and M16 :

$$SST = a_0 + a_1 \times T_{11} + a_2 \times (T_{11} - T_{12}) \times T_{ref} + a_3 \times (T_{11} - T_{12}) \times (\sec\theta_{sat} - 1) \qquad (1)$$

Where T_{11} and T_{12} are the brightness temperatures at M15 (11µm) and M16 (12µm), respectively. T_{ref} is the first guess SST from either numerical weather prediction or analysis fields. a_0, a_1, a_2, and a3 are the coefficients derived from the regression process.

VIIRS SST EDR group found an anomalous striping pattern in daytime SST product, and they developed an algorithm to improve the operational SST imagery. However, we still need to analyze the striping at the SDR or L1b level to reduce the propagation of any system artifacts to SST product. Figure 1 shows striping at SDR brightness temperature.

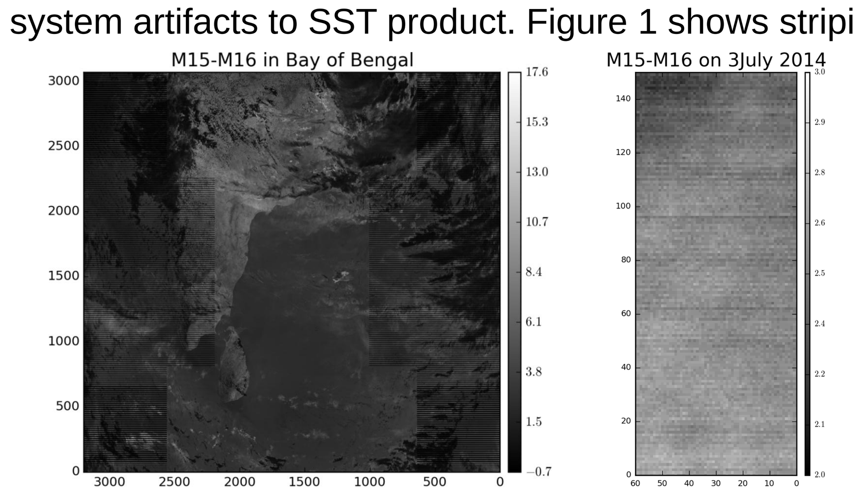

Figure 1. Suomi NPP VIIRS SDR brightness temperature product in M15–M16 over the bay of Bengal on July 3, 2014 (Left); Subset of SDR BT for a uniform ocean surface under clear sky condition.

Line-by-Line Radiative Transfer Model

LBLRTM [*Clough et al. 1981*] is an accurate and efficient line-by-line radiative transfer model which provides spectral radiance calculations with accuracies consistent with the measurements [*Clough et al. 2004*]. LBLRTM 12 is used in this study to simulate the TOA spectral radiance under six standard LBLRTM atmospheric profiles.

The output spectral radiance is then convolved with VIIRS relative spectral response (RSR) to get the channel effective radiance:

$$L_{eff} = \frac{\int_{\nu_1}^{\nu_2} L\, R_\nu\, d\nu}{\int_{\nu_1}^{\nu_2} R_\nu\, d\nu} \qquad (2)$$

where L is the at sensor radiance and R_ν is the RSR of a given band. The simulated effective radiance for each band (L_{eff}) was converted to BT (T_{eff}) using the numerical method by minimizing the difference between BB radiance and channel effective radiance.

In this study, we will check the difference in effective brightness temperature (ΔT_{eff}) [K] between using the detector-level RSR and the band averaged RSR.

$$\Delta T_{eff} = T_{eff\,(\det RSR)} - T_{eff\,(avgRSR)} \qquad (3)$$

Where $T_{eff\,(det\,RSR)}$ is the effective brightness temperature computed using the detector-level RSR and $T_{eff\,(avg\,RSR)}$ is the effective temperature computed using the band averaged RSR.

Model Results

Figure 2 shows the effective brightness temperature differences between the detector-level and band averaged RSR in VIIRS M15 (Top left), M16 (Top right), and M15 – M16 (Bottom) from the LBLRTM radiance output for six atmospheres. Results indicate that there is a small but obvious atmospheric dependency. The odd/even detector pattern is also observed. In M15, the smallest BT difference is at

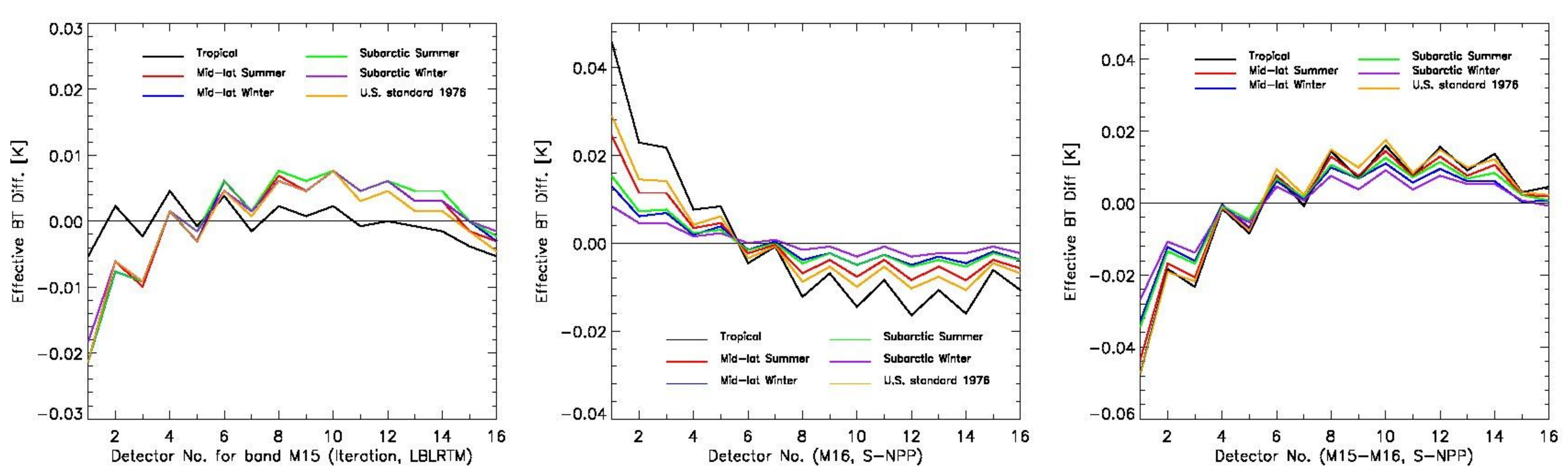

Figure 2. Effective BT difference between detector-level RSR and band averaged Relative Spectral Response using LBLRTM in VIIRS band M15 (Top left), M16 (Top right), and M15 – M16 (Bottom).

The magnitude in effective BT difference among detectors is 0.01K for tropical atmosphere, and 0.025K for subarctic atmosphere (top left panel in Figure 2). To see the impact of spectral range, we extend M15 from [800, 1100] cm^{-1} to the entire spectral range [800, 1333.33] cm^{-1} and M16 from [769, 950] to [769, 1250] cm^{-1} to include the out-of-band response. The results and BT difference patterns are similar as Figure 2 (figure not shown). In M16 (top right panel of Figure 2), there is more obvious atmospheric impact on BT difference than M15, and the tropical atmosphere pattern has the largest variation. Band M16 is more sensitive to water vapor variation due to more water vapor absorption in M16. Detector 6 has the smallest BT difference. Detectors 1 to 6 are more closer to band averaged and then deviate from band average for detectors 8 to 16. For detectors 4 to 16, although Sub-arctic Summer has higher temperature and more water vapor, it has almost same variation as Mid-latitude winter. Therefore, besides water vapor and temperature, other instrument factors may also affect the striping. The term (BT_{15}–BT_{16}) is important because it is used in the VIIRS SST retrieval algorithm. The bottom panel shows that M15–M16 has larger magnitude of variation than single band, for example, they are 0.072K and 0.063K for tropical atmosphere in (M15–M16) and M16, respectively.

Satellite Data Analysis

In order to investigate the relationship between water vapor and striping in VIIRS temperature images, The SDR brightness temperature observation data in band M15 and M16 are analyzed in sample cases from 2012 to 2014. Ten cases over the "uniform" clear sky ocean surface near tropical and polar region are used in this study. In each image, the small uniform region under clear sky conditions was selected based on VIIRS Cloud Mask Intermediate Product (IICMO).

We used the striping index (called SI thereafter) defined in a previous study (Li, 2015) to quantify the striping pattern. The cumulative histogram defined by Li is used to quantify the striping in the image:

$$H_{i,d}(k) = \frac{1}{N_{i,d}} \sum_{l=0}^{k} \left(\sum l \in (l,i,d) \right) \qquad (4)$$

Figure 3. The cumulative histogram for Bay of Bengal over tropical region on June 9, 2013 in M15–M16 (Left), as well as M15 and M16 (Right).

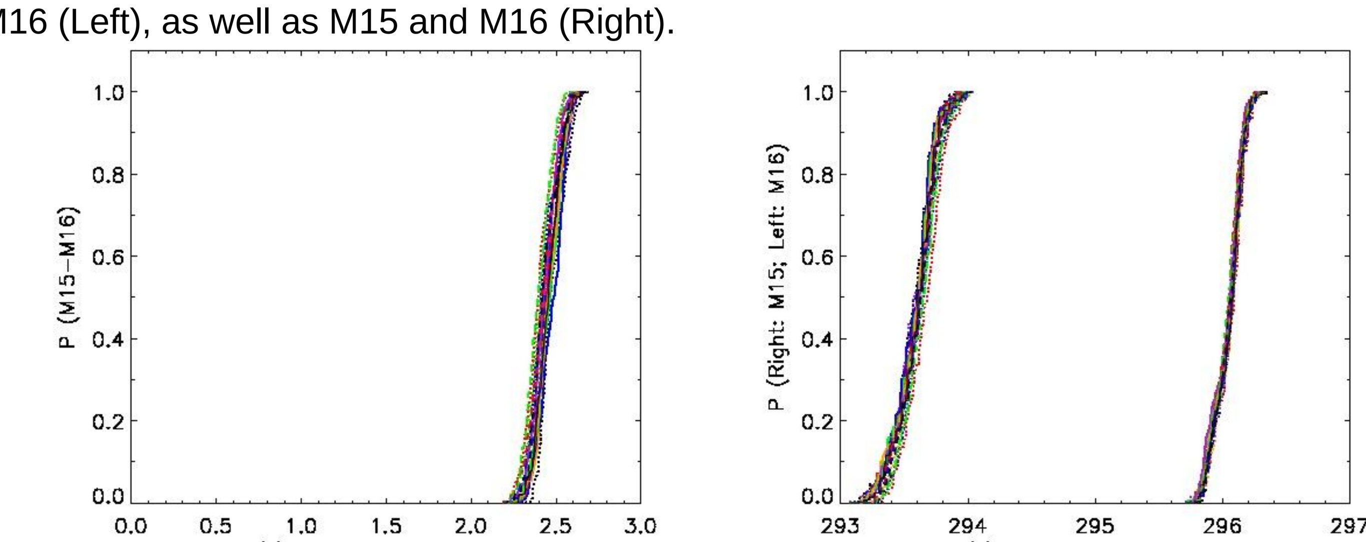

In Figure 3, Y-axis is the percentage of the pixels with value less than the value in X-axis. X-axis represents BT difference in M15–M16 and BT in M15 & M16, respectively. Each line represents one detector. We found that the horizontal distance between histograms is almost a constant. BT_{15}–BT_{16} also represents the water vapor. The left panel also shows that striping does not depend on water vapor within the small water vapor range. The relative magnitude, i.e., the ratio of horizontal distance to the X-axis range is defined as R=g(50%)/Range$_{Xaxis}$. The ratios in M15–M16, M15 and M16 are 0.187, 0.067 and 0.107, respectively. M15–M16 has larger ratio than single band. These horizontal distances are a little bit larger than LBLRTM magnitudes in BT difference for M15–M16, M15, and M16. Over polar regions, the ratios are 0.149, 0.044, and 0.015 for M15-M16, M15, and M16, respectively, which are smaller than those over tropical regions.

The effective BT difference from LBLRTM and VIIRS observation are compared in Figure 4. In M15–M16 and M16, both LBLRTM and VIIRS observation show larger BT difference in tropical than in polar region. In most cases, VIIRS observation has larger magnitude in BT difference among different detectors than LBLRTM except for polar case in M15–M16. In general, the magnitude of variation among 16 detectors over tropical region is much more affected by water vapor than that over polar region, i.e., which is larger for high BT difference (high water vapor absorption). Therefore, the water vapor has impact on the striping pattern, but it is not the dominant factor.

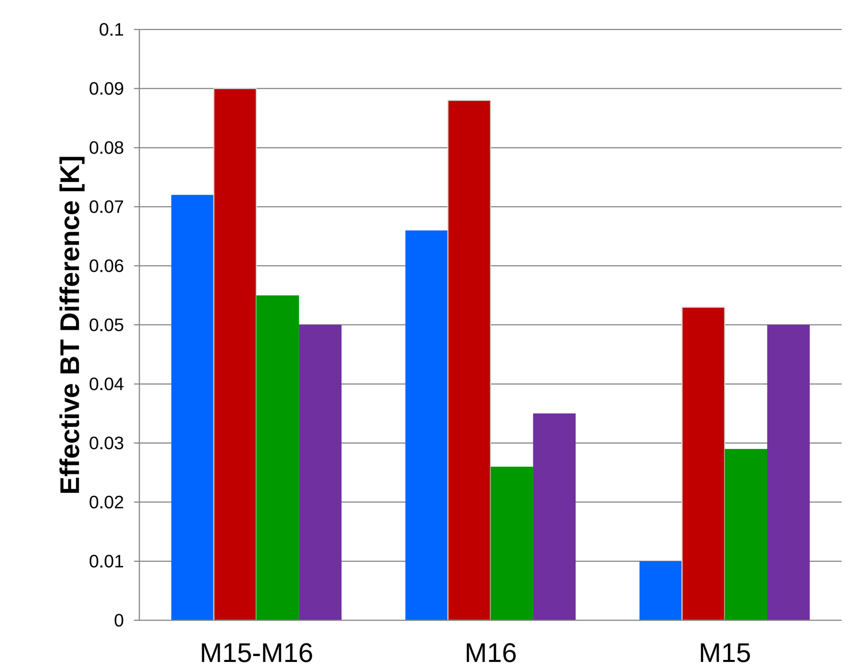

Figure 4. The comparison of effective BT difference between LBLRTM and the VIIRS observation for tropical and polar cases.

Summary

- LBLRTM results show that the striping pattern in VIIRS SST imagery is most likely related to the difference between band averaged RSR and detector level RSR. The effective BT difference has some atmospheric dependency. The results are consistent with MODTRAN results.

- Ten case studies using VIIRS SDR BT observation over tropical and polar regions also show that the detector level difference in tropical region is more obvious than that in polar region. The BT bias is larger for warm and moist atmosphere, but smaller for cold and dry atmosphere. Band M16 is more sensitive to the atmospheric conditions.

- In general, VIIRS SDR BT observation has larger variability when comparing with the model output. It is not easy to effectively validate. The difference due to atmospheric conditions or water vapor is small and not a dominant factor for striping.

- Further study will focus on detector stability and fixed pattern noise.

Acknowledgement: Thanks Yan Bai for providing sample data.

References

Clough, S.A., Kneizys, F.X., Rothman, L.S., Gallery, W.O. (1981), Atmospheric spectral transmittance and radiance: FASCOD1B. *Proc Soc Photo Opt Instrum Eng*, Vol. 277, 152–166.

Clough, S.A., M.W. Shephard, E.J. Mlawer, J.S. Delamere, M.J. Iacono, K. Cady-Pereira, S. Boukabara, P.D. Brown (2005), Atmospheric radiative transfer modeling: a summary of the AER codes, J. Quantitative Spectroscopy & Radiative Transfer, Vol. 91, 233 –244.

Dash, P., and A. Ignatov (2008), Validation of clear-sky radiances over oceans simulated with MODTRAN4.2 and global NCEP GDAS fields against nighttime NOAA15-18 and MetOp-A AVHRR data, *Remote Sens. Environ.*, *112*, 3012-3029, doi:10.1016/j.rse.2008.02.013.

Francis Padula and Changyong Cao (2015), Detector-Level Spectral Characterization of the Suomi NPP VIIRS Long-Wave Infrared Bands M15 & M16. Applied Optics.

Li, Zhenping, 2015: Real Time De-Striping Algorithm for Geostationary Operational Environmental Satellite (GOES) P Sounder Images.